A Neural Network Architecture for Preattentive Vision

STEPHEN GROSSBERG, ENNIO MINGOLLA, AND DEJAN TODOROVIĆ

(*Invited Paper*)

Abstract—**Recent results towards development of a neural network architecture for general-purpose preattentive vision are summarized. The architecture contains two parallel subsystems, the boundary contour system (BCS) and the feature contour system (FCS), which interact together to generate a representation of form-and-color-and-depth. Emergent boundary segmentation within the BCS and featural filling-in within the FCS are herein emphasized within a monocular setting. Applications to the analysis of boundaries, textures, and smooth surfaces are described, as is a model for invariant brightness perception under variable illumination conditions. The theory shows how suitably defined parallel and hierarchical interactions overcome computational uncertainties that necessarily exist at early processing stages. Some of the psychophysical and neurophysiological data supporting the theory's predictions are mentioned.**

The Need for a General Purpose Preattentive Vision Machine

MANY AI algorithms for machine vision have been too specialized for applications to real-world problems. Such algorithms are often designed to deal with one type of information—for example, boundary, disparity, curvature, shading, or spatial frequency information. Moreover, such algorithms typically use different computational schemes to analyze each distinct type of information, so that unification into a single general-purpose vision algorithm is difficult at best. For such AI algorithms, other types of signals are often contaminants, or noise elements, rather than cooperative sources of ambiguity-reducing information. Unfortunately, most realistic scenes contain partial information of several different types in each part of a scene.

In contrast, when we humans gaze upon a scene, our brains rapidly combine several different types of locally ambiguous visual information to generate a globally consistent and unambiguous representation of form-and-color-in-depth. This state of affairs raises the question: what new computational principles and mechanisms are needed to understand how multiple sources of visual information cooperate automatically to generate a percept of three-dimensional form?

The Center for Adaptive Systems at Boston University has been developing such a general purpose automatic vision architecture, and this paper reviews and integrates some of our recent work on its design. This architecture clarifies how scenic data about boundaries, textures, shading, depth, multiple spatial scales, and motion can be cooperatively synthesized in real-time into a coherent representation of three-dimensional form. Moreover, it has become clear through cooperative work with collegues at M.I.T. Lincoln Laboratory that the same processes which are useful to automatically process visual data from human sensors are equally valuable for processing noisy multidimensional data from artificial sensors, such as laser radars. These processes are called emergent segmentation and featural filling-in.

Manuscript received January 29, 1988; revised July 5, 1988. This work was supported by the Air Force Office of Scientific Research Grants AFOSR F49620-86-C-0037, F49620-87-C-0018, and F49620-87-C-0018; the Army Research Office Grants DAAG-29-85-K-0095 and DAAG-29-85-K-0095; and the National Science Foundation Grant IRI-84-17756.

S. Grossberg and E. Mingolla are with the Center For Adaptive Systems, Boston University, Boston, MA 02215.

D. Todorović is with the Labroatoriha za Eksperimentalnu Psihologihu, Univerzitet u Beogradu, 11000 Beograd, Yugoslavia.

IEEE Log Number 8824418.

Why do We Bother to See? The Difference Between Seeing and Recognizing

The difficulties inherent in computationally understanding biological vision can be appreciated by considering a few examples. Fig. 1 depicts a type of visual image that has been named after L. Glass. When we view such a Glass pattern, we *see* and *recognize* many black dots on white paper, but we also *recognize* among the dots circular groupings that we do not *see*. For most individuals, these circular groupings do not generate brightnesses or colors that differ significantly from the background. Thus there is a profound difference between seeing and recognizing, and we can sometimes recognize groupings that we cannot see. This state of affairs raises the interesting question: if we can recognize things that we cannot see, then why do we bother to see?

The seriousness of this issue is illustrated by considering the image of a texture shown in Fig. 2, which was introduced by Beck [1]. Humans can very quickly, and without prior experience with that texture, distinguish its top-half from its bottom-half. One type of factor that we use to accomplish this are the long horizontal groupings which are generated perpendicular to the line ends in the top half of the texture. Although these emergent horizontal groupings, or segmentations, are critical in helping us to *recognize* that the bottom half is different from the top half, these horizontal segmentations are not *seen* in the traditional sense of generating a large brightness or color differences. Thus, perceptually invisible segmentations are critical in the recognition of visual form.

The other side of the coin is equally perplexing; namely, we can sometimes see things that are not in the image, as

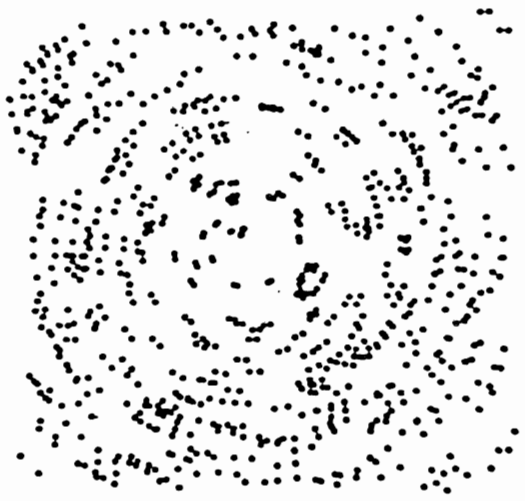

Fig. 1. A glass pattern: the emergent circular pattern is "recognized," although it is not "seen," as a pattern of differing contrasts. The text suggests how this happens.

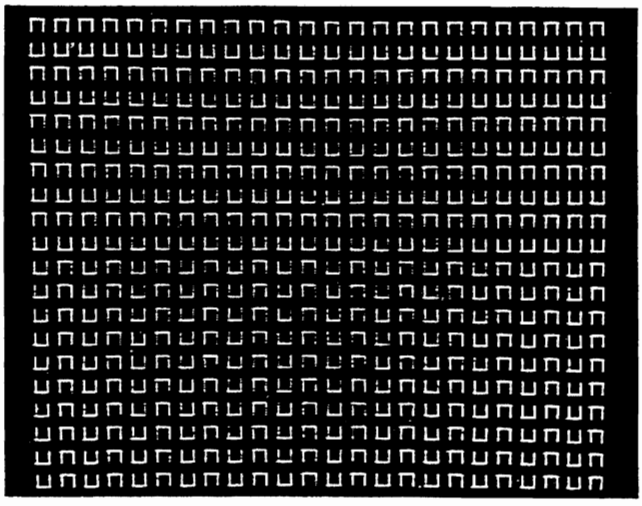

Fig. 2. Textural grouping supported by subjective contours: cooperation among end cuts induced perpendicular to the image line ends generates horizontal subjective contours in the top half of this figure. The text suggests how this happens.

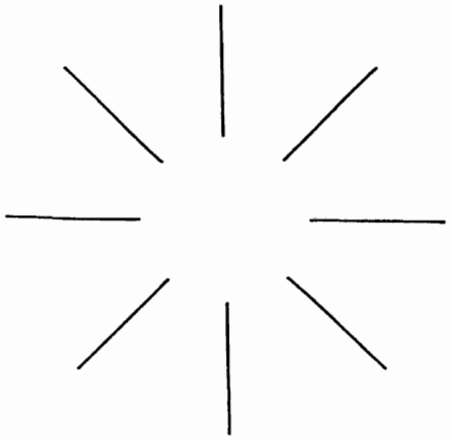

Fig. 3. An Ehrenstein figure: a bright circular disk is perceived even though all white areas are equally luminant. The text suggests how this happens.

in illusory figures. Thus, in viewing the Ehrenstein figure shown in Fig. 3, we can see a bright disk within the perpendicular lines, although the luminance across all white parts of the figure is the same.

The Hierarchical Resolution of Uncertainty

In order to computationally understand such labile relationships between recognized emergent segmentations and seen brightnesses, it has been necessary to develop a qualitatively different type of vision theory [6], [10]–[13], [15]. Our theory holds that the seeming paradoxes of Figs. 1–3 can be understood by considering such figures to be probes of adaptive neural mechanisms which evolved as our ancestors coped with constantly changing visual environments. Specifically, our visual systems are designed to detect relatively invariant surface colors under variable illumination conditions, to detect relatively invariant object boundary structures amid noise caused by the eyes' own optics or occluding objects, and to recognize familiar objects or events in the environment. These three principle functions are performed by the three main subsystems of our theory, the feature contour system (FCS), the boundary contour system (BCS), and the object recognition system (ORS), respectively, as indicated in the macrocircuit of Fig. 4.

A unifying theme constraining the design of the theory's mechanisms is that there exist fundamental limitations of the visual measurement process—that is, uncertainty principles are just as important in vision as in quantum mechanics. For example, the computational demands placed on a system that is designed to detect invariant surface colors are, in many respects, complementary to the demands placed on a system that is designed to detect invariant boundary structures. That is why the FCS and BCS in Fig. 4 process the signals from each monocular preprocessing (MP) stage in parallel. This is not to say that the FCS and BCS are independent modules. Fig. 5 depicts in greater detail how levels of the FCS and BCS interact through multiple feedforward and feedback pathways to generate a visual representation at the final level of the FCS, which is called the binocular syncytium.

In addition to the complementary relationship between the FCS and the BCS, there also exist informational uncertainties at processing levels within each of these systems. As indicated below, the computations within the FCS which reduce uncertainty due to variable illumination conditions create new uncertainties about surface brightnesses and colors that are resolved at a higher FCS level by a process of featural filling-in. Likewise, the computations within the BCS which reduce uncertainty about boundary orientation create new uncertainties about boundary position that are resolved at a higher BCS level by a process of boundary completion.

The theory hereby describes how the visual system as a whole can compensate for such uncertainties using both parallel and hierarchical stages of neural processing. Thus the visual system is designed to achieve *heterarchical compensation for uncertainties of measurement.*

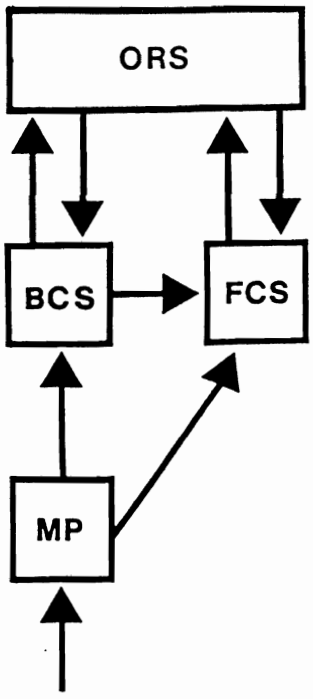

Fig. 4. A macrocircuit of processing stages: monocular preprocessed signals (MP) are sent independently to both the boundary contour system (BCS) and the feature contour system (FCS). The BCS preattentively generates coherent boundary structures from these MP signals. These structures send outputs to both the FCS and the object recognition system (ORS). The ORS, in turn, rapidly sends top-down learned template signals, or expectations, to the BCS. These template signals can modify the preattentively completed boundary structures using learned, attentive information. The BCS passes these modifications along to the FCS. The signals from the BCS organize the FCS into perceptual regions wherein filling-in of visible brightnesses and colors can occur. This filling-in process is activated by signals from the MP stage. The completed FCS representation, in turn, also interacts with the ORS.

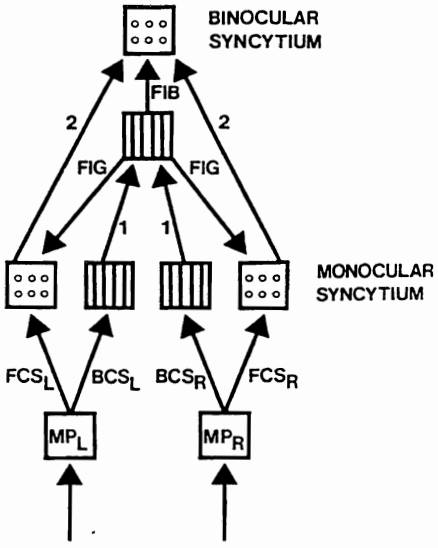

Fig. 5. Macrocircuit of monocular and binocular interactions within the boundary contour system (BCS) and the feature contour system (FCS): left and right monocular preprocessing stages (MP_L and MP_R) send parallel monocular inputs to the BCS (boxes with vertical lines) and the FCS (boxes with three pairs of circles). The monocular BCS_L and BCS_R interact via bottom-up pathways labeled 1 to generate a coherent binocular boundary segmentation. This segmentation generates output signals called filling-in generators (FIG's) and filling-in barriers (FIB's). The FIGs input to the monocular filling-in domains, or syncytia, of the FCS. The FIB's input to the binocular filling-in domains, or syncytia, of the FCS. Inputs from the MP stages interact with FIG's at the monocular syncytia where they select those monocular FC signals that are binocularly consistent. The selected FC signals are carried by the pathways labeled 2 to the binocular syncytia where they interact with FIB signals from the BCS to generate a multiple scale representation of form-and-color-in-depth within the binocular syncytia. The present article describes some monocular properties of the interactions from an MP stage through the first few BCS and FCS stages, namely those symbolized by the pathways labeled 1 and FIG.

One of the theory's most central and novel insights consists in the interactions which it posits between the BCS and the FCS. The division of labor described so far—the BCS to perform boundary segmentation and the FCS to detect verdical surface color—is not simply a partitioning for simplicity or convenience. Rather, the real-time computational demands of the two processes are intimately related and in specific ways. As shown below, BCS dynamics require oriented filtering operations followed by oriented cooperative-competitive feedback interactions because such an architecture can rapidly and in a context-sensitive manner perform the requisite boundary segmentation that the FCS itself needs in order to pool, or fill-in, its estimates of surface color among regions belonging to the same perceived objects. That pooling is a type of unoriented spatial averaging performed by a diffusion process which is described in a subsequent section. Were a diffusion of signals employed within the BCS itself, however, it could blur the very boundaries that it seeks to sharpen and thereby defeat both the BCS and FCS system goals. Accordingly, as shown in Fig. 4, the BCS processes occur separately of, and in parallel with, FCS processes, but send topographically matched signals to the FCS to organize the spatial structuring of FCS processes.

The theory's novelty is indicated by the types of paradoxical statements that it makes computationally precise. Thus, not only are the circular and horizontal segmentations of Figs. 1 and 2 invisible, but also *all boundaries are invisible*. Not only are such apparent curiosities as the bright disk in Fig. 3 "illusory" percepts, but even rather mundane objects are "illusory" percepts. Indeed, as explained below, all line ends are illusory.

With this overview, we can now consider the dynamics of these two systems and their relationship to the ORS in greater detail.

Preattentive Visual Processing by the Boundary Contour System and Feature Contour System

The theory's general purpose capabilities depend upon its decomposition into BCS, FCS, and ORS subsystems. Both the BCS and FCS operate preattentively and automatically upon all images, whether or not these images have been experienced before. Unlike approaches based upon simulated annealing [8], [18], the BCS and FCS do not need to include specific information in the form of probability distributions about a limited class of expected images. Moreover, the BCS does not rely upon the independent manipulation of an external parameter, such as a temperature parameter, to regular convergence to an equilibrium determined by these predetermined probability

distributions. Instead the BCS utilizes internal cooperative–competitive feedback interactions to regulate the real-time grouping and convergence of the system to one of a very large number of possible stable equilibria. Consequently, whereas stochastic relaxation techniques can, at best, sharpen expected properties of an image, the BCS can begin to simulate the key property of preattentive vision: the automatic discovery of emergent image groupings that may never have been experienced before.

Thus, the BCS is itself a general purpose device in the sense that it can generate an emergent 3-D boundary segmentation in response to a wide variety of image properties. For example, it is capable of detecting, sharpening, and completing image edges; of grouping textures; of generating a boundary web of boundary compartments that conform to the shape of smoothly shaded regions; and of carrying out a disparity-sensitive and scale-sensitive binocular matching process that generates fused binocular structures from disparate pairs of monocular images. The outcome of this 3-D boundary segmentation process is perceptually invisible within the BC System. Visible percepts are a property of the FC System.

A completed segmentation within the BC system elicits topographically organized output signals to the FC system. These completed BC signals regulate the hierarchical processing of color and brightness signals by the FC system (Fig. 5). Notable among FC system processes are the automatic extraction from many different types of images of color and brightness signals that are relatively uncontaminated by changes in illumination conditions—again a general purpose property. These feature contour signals interact within the FC system with the output signals from the BC system to control featural filling-in processes. These filling-in processes lead to visible percepts of color-and-form-in-depth at the final stage of the FC system, which is called the binocular syncytium (Fig. 5).

Such a theoretical decomposition of the vision process conforms to, and has in fact predicted, properties of a similar decomposition that governs the design of the mammalian visual cortex. For example, in the theory's analyses and predictions of neurobiological data, the monocular preprocessor stage (MP_L, MP_R) of Figs. 4 and 5 is compared with opponent cells of the lateral geniculate nucleus, the first stage of the BC system is compared with simple cells of the hypercolumns in area $V1$ of striate cortex, the first stage of the FC system is compared with cells of the cytochrome oxydase staining blobs of area $V1$ of striate cortex, the binocular syncytium is compared with cells of area $V4$ of the prestriate cortex, and the intervening BC system and FC system stages are compared with complex, hypercomplex, double opponent, and related cell types in areas $V1$, $V2$, and $V4$ of striate and prestriate cortex [10], [12]. Some of these neural interpretations are described in greater detail in subsequent sections.

Interactions Between Preattentive Vision and Postattentive Learned Object Recognition

The processes summarized in Figs. 4 and 5 are preattentive and automatic. These preattentive processes may, however, influence and be influenced by attentive, learned object recognition processes. The macrocircuit depicted in Fig. 4 suggests, for example, that a preattentively completed boundary segmentation within the BCS can directly activate an object recognition system (ORS), whether or not this segmentation supports visible contrast differences within the FCS. In the Glass pattern of Fig. 1, for example, the circular groupings can be recognized by the ORS even though they do not support visible contrast differences within the FCS.

The ORS can, in turn, read out attentive learned priming, or expectation, signals to the BCS. Why the ORS needs to read out learned top-down attentive feedback signals is clarified elsewhere by results from adaptive resonance theory, which has demonstrated that learned top-down expectations help to stabilize the self-organization of object recognition codes in response to complex and unpredictable input environments [3]–[5]. In response to familiar objects in a scene, the final 3-D boundary segmentation within the BCS may thus be *doubly* completed, first by automatic preattentive segmentation processes and then by attentive learned expectation processes. This doubly completed segmentation regulates the featural filling-in processes within the FCS that lead to a percept of visible form. The FCS also interacts with the ORS in order to generate recognitions of color and surface properties.

The feedback interactions between the preattentive BCS and FCS and the attentive, adaptive ORS emphasize that these subsystems are not independent modules, and clarify why the distinction between preattentive and attentive visual processing has been so controversial and elusive in the vision literature. Indeed, while seminal workers such as Beck and Julesz have probed the preattentive aspects of textural grouping, no less distinguished work, using closely related visual images, has emphasized the attentive and cognitive aspects of vision, as in the "unconscious inferences" of Helmholtz and the "cognitive contours" of Gregory. The possibility that emergent segmentations within the BCS can be doubly completed, both by preattentive segmentations and attentive learned expectations, helps to unify these parallel lines of inquiry, and cautions against ignoring the influence of attentive feedback upon the "preattentive" BCS and FCS. In addition, the rules whereby such parallel inputs from the BCS and the FCS are combined within the ORS have recently been the subject of active experimental investigation, especially due to the excitement surrounding the discovery of "illusory conjunctions" [26], whereby form and color information may be improperly joined under suitable experimental conditions.

The functional distinction between the attentive learned ORS and the "preattentive" BCS and FCS also has a neural analog in the functional architecture of mammalian neocortex. Whereas the BCS and FCS are neurally interpreted in terms of data about areas $V1$, $V2$, and $V4$ of visual cortex, the ORS is interpreted in terms of data concerning inferotemporal cortex and related brain regions [23].

The present theory hereby clarifies two distinct types of

interactions that may occur among processes governing form and color perception: preattentive interactions from the BCS to the FCS (Fig. 5) and attentive interactions between the BCS and the ORS and the FCS and the ORS (Fig. 4). We now summarize the monocular model mechanisms whereby the BCS and the FCS preattentively interact. This foundation has elsewhere been used to derive the theory's binocular mechanisms [11].

Discounting the Illuminant: Extracting Feature Contours

One form of uncertainty with which the nervous system deals is due to the fact that the visual world is viewed under variable lighting conditions. When an object reflects light to an observer's eyes, the amount of light energy within a given wavelength that reaches the eye from each object location is determined by a product of two factors. One factor is a fixed ratio, or reflectance, which determines the fraction of incident light that is reflected by that object location to the eye. The other factor is the variable intensity of the light which illuminates the object location. Two object locations with equal reflectances can reflect different amounts of light to the eye if they are illuminated by different light intensities. Spatial gradients of light across a scene are the rule, rather than the exception, during perception, and wavelengths of light that illuminate a scene can vary widely during a single day. If the nervous system directly coded into percepts the light energies which it received, it would compute false measures of object colors and brightnesses, as well as false measures of object shapes. This problem was already clear to Helmholtz. It demands an approach to visual perception that points away from a simple Newtonian analysis of colors and white light.

Land [19] and his colleagues have sharpened contemporary understanding of this issue by carrying out a series of remarkable experiments. In these experiments, a picture constructed from overlapping patches of colored paper, called a McCann Mondrian, is viewed under different lighting conditions. If red, green, and blue lights simultaneously illuminate the picture, then an observer perceives surprisingly little color change as the intensities of illumination are chosen to vary within wide limits. The stability of perceived colors obtains despite the fact that the intensity of light at each wavelength that is reflected to the eye varies linearly with the incident illumination intensity at that wavelength. This property of color stability indicates that the nervous system "discounts the illuminant," or suppresses the "extra" amount of light in each wavelength, in order to extract a color percept that is invariant under many lighting conditions.

In an even more striking experimental demonstration of this property, inhomogeneous lighting conditions were devised such that spectrophotometric readings from positions within the interiors of two color patches were the same, yet the two patches appeared to have different colors. The perceived colors were, moreover, close to the colors that would be perceived when viewed in a homogeneous source of white light.

These results show that the signals from within the interiors of the colored patches are significantly attenuated in order to discount the illuminant. This property makes ecological sense since even a gradual change in illumination level could cause a large cumulative distortion in perceived color or brightness if it were allowed to influence the percept of a large scenic region. In contrast, illuminant intensities typically do not vary much across a scenic edge. Thus, the ratio of light signals reflected from the two sides of a scenic edge can provide an accurate local estimate of the relative reflectances of the scene at the corresponding positions. We have called the color and brightness signals which remain unattenuated near scenic edges FC signals.

The neural mechanisms which "discount the illuminant" overcome a fundamental uncertainty in the retinal pickup of visual information. In so doing, however, they create a new problem of uncertain measurement, which illustrates one of the classical uncertainty principles of visual perception. If color and brightness signals are suppressed except near scenic edges, then why do not we see just a world of colored edges? How are these local FC signals used by later processing stages to synthesize global percepts of continuous forms, notably of color fields and of smoothly varying surfaces?

Featural Filling-In and Stabilized Images

Our monocular theory has developed mechanisms whereby contour-sensitive FC signals activate a process of lateral spreading, or filling-in, of color and brightness signals within the FCS. This filling-in process is contained by topographically organized output signals from the BCS to the FCS (Fig. 5). Where no BC signals obstruct the filling-in process, its strength is attenuated with distance since it is governed by a nonlinear diffusion process. Our monocular model for this filling-in process was developed and tested using quantitative computer simulations of paradoxical brightness data.

Many examples of featural filling-in and its containment by BC signals can be cited. A classical example of this phenomenon is described in Fig. 6. The image in Fig. 6 was used by Yarbus [28] in a stabilized image experiment. Normally, the eye jitters rapidly in its orbit, and thereby is in continual relative motion with respect to a scene. In a stabilized image experiment, prescribed regions in an image are kept stabilized, or do not move with respect to the retina. Stabilization is accomplished by the use of a contact lens or an electronic feedback circuit. Stabilizing an image with respect to the retina can cause the perception of the image to fade. The adaptive utility of this property can be partially understood by noting that, in humans, light passes through retinal veins before it reaches the photosensitive retina. The veins form stabilized images with respect to the retina; hence, they are fortunately not visible under ordinary viewing conditions.

In the Yarbus display shown in Fig. 6, the large circular edge and the vertical edge are stabilized with respect to the retina. As these edge percepts fade, the red color outside the large circle is perceived to flow over and envelope

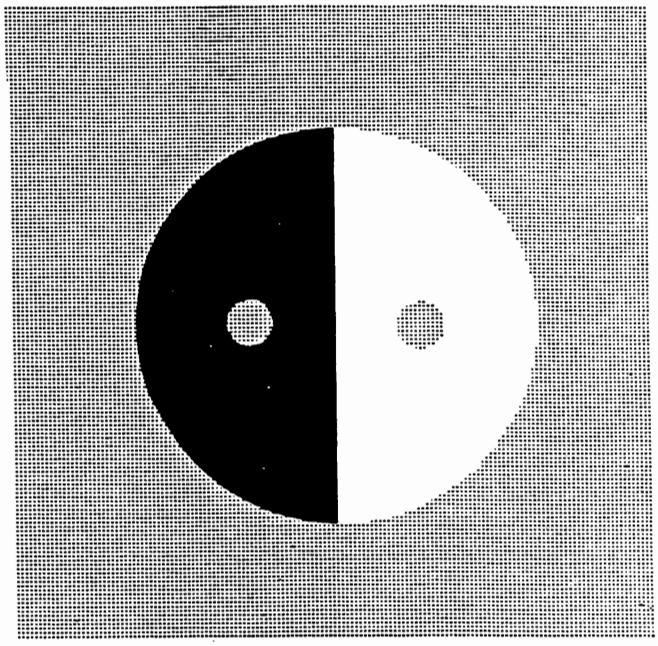

Fig. 6. A classical example of featural filling-in: when the edges of the large circle and the vertical line are stabilized on the retina, the red color (dots) outside the large circle envelopes the black and white hemidisks except within the small red circles whose edges are not stabilized [28]. The red inside the left circle looks brighter and the red inside the right circle looks darker than the enveloping red.

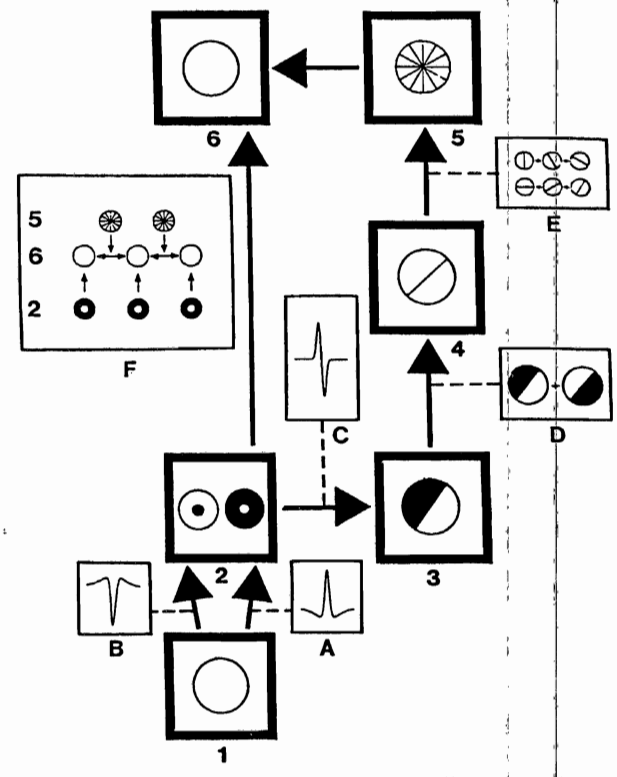

Fig. 7. Model of how the feature contour system discounts variable illuminants and regulates featural filling-in: The thick-bordered rectangles numbered from 1 to 6 correspond to the levels of the system. The symbols inside the rectangles are graphical mnemonics for the types of computational units residing at the corresponding model level. The arrows depict the interconnections between the levels. The thin-bordered rectangles coded by letters A through E represent the type of processing between pairs of levels. Inset F illustrates how the activity at level 6 is modulated by outputs from level 2 and level 5. This simplified model directly extracts boundaries from image contrasts, rather than generating emergent segmentations from image contrasts. The model's key elements concern how the level 2 network of shunting on-center off-surround interactions discounts variable illuminants while extracting feature contour signals, and how level 5 fills-in these signals via a nonlinear diffusion process within the compartments defined by boundary contour system output signals.

the black and white hemi-discs until it reaches the small red circles whose edges are not stabilized. This percept illustrates how FC signals can spread across, or fill-in, a scenic percept until they hit perceptually significant boundaries. Our neural network model of this process explains how filling-in occurs within the black and white regions, and why the left red disk appears lighter and the right red disk appears darker than the surrounding red region that envelopes the remainder of the percept.

This model is schematized in Fig. 7. It has been used to simulate a wide range of classical and recent phenomena concerning brightness perception which have not heretofore been explained by a single theory [15]. The equations defining the model are now defined.

A Model for Invariant Brightness Perception Under Variable Illumination Conditions

The equations underlying the Grossberg and Todorović [15] model are based on and extend work by Grossberg [9], Cohen and Grossberg [6], and Grossberg and Mingolla [13]. The exposition follows the description of levels in Fig. 7. Only the two-dimensional versions of the equations are presented. The one-dimensional forms can be derived by straightforward simplifications. The two-dimensional simulation in Fig. 9 below was performed on a 30 × 30 lattice and that in Fig. 10 on a 40 × 40 lattice. The one-dimensional simulations involve 256 units.

Level 1: Gray-Scale Image Description

Denote by I_{ij} the value of the stimulus input at position (i, j) in the lattice. In all simulations these values varied between 1 and 9. In order to compute the spatial convolutions of level 2 cells without causing spurious edge effects at the extremities of the luminance profile, the luminance values at the extremities were continued outward as far as necessary.

Level 2: Shunting On-Center Off-Surround Network for Discounting Illuminants and Extracting FC Signals

The activity x_{ij} of a level 2 on-cell at position (i, j) of the lattice obeys a membrane equation, also called a shunting equation,

$$\frac{d}{dt}x_{ij} = -Ax_{ij} + (B - x_{ij})C_{ij} - (x_{ij} + D)E_{ij} \quad (1)$$

where $C_{ij}(E_{ij})$ is the total excitatory (inhibitory) input to x_{ij}. Each input C_{ij} and E_{ij} is a discrete convolution with Gaussian kernel of the inputs I_{pq}:

$$C_{ij} = \sum_{(p,q)} I_{pq}C_{pqij} \quad (2)$$

and

$$E_{ij} = \sum_{(p,q)} I_{pq} E_{pqij} \tag{3}$$

where

$$C_{pqij} = C \exp\left\{-\alpha^{-2} \log 2\left[(p-i)^2 + (q-j)^2\right]\right\} \tag{4}$$

and

$$E_{pqij} = E \exp\left\{-\beta^{-2} \log 2\left[(p-i)^2 + (q-j)^2\right]\right\}. \tag{5}$$

The influence exerted on the level 2 potential x_{ij} by input I_{pq} diminishes with increasing distance between the two corresponding locations. Thus, the receptive fields have a circular shape. To achieve an on-center off-surround anatomy, coefficient C of the excitatory kernel in (4) is chosen larger than coefficient E of the inhibitory kernel in (5), but α, the radius of the excitatory spread at half strength in (4), is chosen smaller than β, its inhibitory counterpart in (5). In the simulations, this equation is solved at equilibrium. Then $(d/dt)x_{ij} = 0$, so that

$$x_{ij} = \frac{\sum_{(p,q)} (BC_{pqij} - DE_{pqij}) I_{pq}}{A + \sum_{(p,q)} (C_{pqij} + E_{pqij}) I_{pq}}. \tag{6}$$

The denominator term normalizes the activity x_{ij}.

The output signal from level 2 is the nonnegative, or rectified, part of x_{ij}:

$$X_{ij} = \max(x_{ij}, 0). \tag{7}$$

Levels 3–5 compute the boundary contour signals used to contain the featural filling-in process. These boundary contour signals do not include properties of emergent segmentation. The equations for the BCS may be appended to the model, as explained below, when emergent segmentation is required.

Level 3: Simple Cells

The potential y_{ijk} of the cell centered at position (i, j) whose oriented receptive field possesses orientation k obeys an additive equation

$$\frac{d}{dt} y_{ijk} = -y_{ijk} + \sum_{(p,q)} X_{pq} F^{(k)}_{pqij} \tag{8}$$

which is computed at equilibrium:

$$y_{ijk} = \sum_{(p,q)} X_{pq} F^{(k)}_{pqij} \tag{9}$$

in all our simulations. In order to generate an oriented kernel $F^{(k)}_{pqij}$ as simply as possible, let $F^{(k)}_{pqij}$ be the difference of an isotropic kernel G_{pqij} centered at (i, j) and another isotropic kernel $H^{(k)}_{pqij}$ whose center $(i + m_k, j + n_k)$ is shifted from (i, j) as follows:

$$F^{(k)}_{pqij} = G_{pqij} - H^{(k)}_{pqij} \tag{10}$$

where

$$G_{pqij} = \exp\left\{-\gamma^{-2}\left[(p-i)^2 + (q-j)^2\right]\right\} \tag{11}$$

and

$$H^{(k)}_{pqij} = \exp\left\{-\gamma^{-2}\left[(p-i-m_k)^2 + (q-j-n_k)^2\right]\right\} \tag{12}$$

with

$$m_k = \sin\frac{2\pi k}{K} \tag{13}$$

and

$$n_k = \cos\frac{2\pi k}{K}. \tag{14}$$

In the 2-D simulations, the number K is 12, whereas for the 1-D simulations it is 2.

The output signal from level 3 to level 4 is the nonnegative, or rectified, part of y_{ijk}, namely

$$Y_{ijk} = \max(y_{ijk}, 0). \tag{15}$$

Level 4: Complex Cells

Each level 4 potential z_{ijk} with position (i, j) and orientation k is made sensitive to orientation but insensitive to direction-of-contrast by summing the output signals from the appropriate pair of level 3 units with opposite contrast sensitivities; viz.,

$$z_{ijk} = Y_{ijk} + Y_{ij(k+K/2)}. \tag{16}$$

An output signal Z_{ijk} is generated from level 4 to level 5 if the activity z_{ijk} exceeds the threshold L:

$$Z_{ijk} = \max(z_{ijk} - L, 0). \tag{17}$$

Level 5: Boundary Contour Signals

A level 5 signal z_{ij} at position (i, j) is the sum of output signals from all level 4 units at that position; viz.,

$$Z_{ij} = \sum_k Z_{ijk}. \tag{18}$$

Level 6 computes the filling-in process, which is regulated by feature contour inputs from level 2 and boundary contour inputs from level 5.

Level 6: Filling-In Process

Each potential S_{ij} at position (i, j) of the filling-in process obeys a nonlinear diffusion equation

$$\frac{d}{dt} S_{ij} = -MS_{ij} + \sum_{(p,q)\in N_{ij}} (S_{pq} - S_{ij}) P_{pqij} + X_{ij}. \tag{19}$$

The diffusion coefficients that regulate the magnitude of cross influence of location (i, j) with location (p, q) depend on the boundary contour signals Z_{pq} and Z_{ij} as fol-

lows:

$$P_{pqij} = \frac{\delta}{1 + \epsilon(Z_{pq} + Z_{ij})}. \tag{20}$$

The set N_{ij} of locations comprises only the lattice nearest neighbors of (i, j):

$$N_{ij} = \{(i, j-1), (i-1, j), (i+1, j), (i, j+1)\}. \tag{21}$$

At lattice edges and corners, this set is reduced to the set of existing neighbors. According to (19), each potential S_{ij} is activated by the feature contour output signal X_{ij} and thereupon engages in passive decay (term $-MS_{ij}$) and diffusive filling-in with its four nearest neighbors to the degree permitted by the diffusion coefficients P_{pqij}. At equilibrium, each S_{ij} is computed as the solution of a set of simultaneous equations

$$S_{ij} = \frac{X_{ij} + \sum_{(p,q)\in N_{ij}} S_{pq} P_{pqij}}{M + \sum_{(p,q)\in N_{ij}} P_{pqij}} \tag{22}$$

which is compared with properties of the brightness percept. See Grossberg and Todorović [15] for parameter choices.

Computer Simulations of Brightness Constancy, Contrast, and Assimilation

Fig. 8 depicts the results of four computer simulations with a single set of parameters using a one-dimensional version of the model to illustrate its responses to images which possess a one-dimensional symmetry. In such an image, each horizontal slice through the image possesses the same luminance profile, labeled stimulus in Fig. 8. Fig. 8(a) and (b) illustrate discounting the illuminant and brightness constancy; Fig. 8(c) illustrates discounting the illuminant and brightness contrast; and Fig. 8(d) illustrates brightness assimilation. Note that the feature contour patterns, labeled feature, are distributed activation patterns with positive baseline values, rather than zero crossings, binary edge patterns, or other classical objects. Comparison of the feature contour patterns of Fig. 8(a) and (b) illustrate how these patterns discount the illuminant. The theory also explains how a feature contour pattern triggers a filling-in, or diffusion, process within compartments bounded by a boundary contour pattern, labeled boundary, to generate the filled-in pattern, labeled output, on which the percept is based.

Visible Effects of Invisible Causes

The computer simulation summarized in Fig. 8(c) is of particular interest because it illustrates a visible effect of an invisible cause. The luminance gradient between the two equiluminant patches in the stimulus caused the different brightnesses of these patches in the output, but is

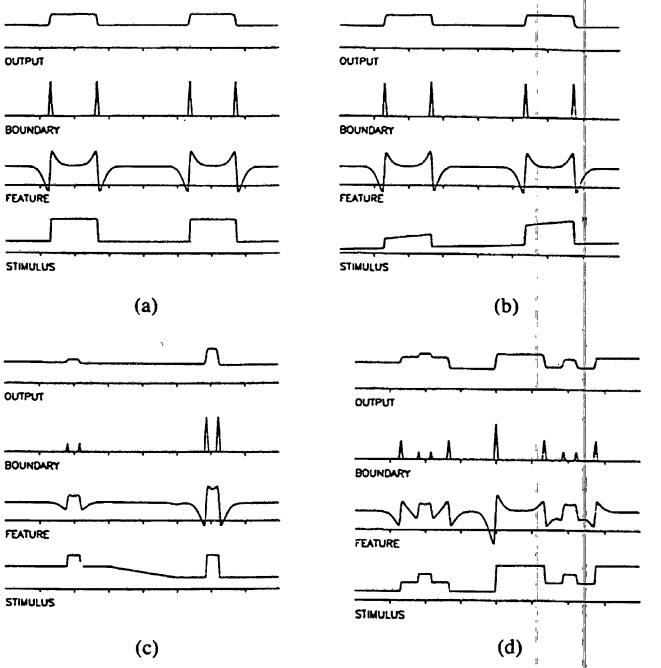

Fig. 8. Simulation of feature contour interactions in response to images with a one-dimensional symmetry: the luminance profile (stimulus) in (b) is tilted with respect to that in (a) due to an asymmetric light source, but the filled-in percept (output) is the same as that in (a), illustrating discounting of the illuminant and brightness constancy. Although the small patches have equal luminance in (c), their filled-in percepts are different, in the direction opposite to their backgrounds, illustrating brightness contrast. Although the small inner patches have equal luminance in (d), the filling-in percept of the right patch is darker than that of the left patch, in the direction of their surrounding patches, illustrating brightness assimilation.

itself rendered invisible in the output due to filling-in. Such a process helps to explain the percept of the Yarbus display in Fig. 6, which also includes a visible contrast due to an invisible filled-in image property.

Simulation of Craik-O'Brien Cornsweet and McCann Mondrian Percepts

Figs. 9 and 10 show the results of computer simulations using the full two-dimensional version of the model. These simulations suggest an explanation of two important visual phenomena which are partly due to featural filling-in: the Craik-O'Brien Cornsweet effect and a McCann Mondrian image in response to which humans perceive a brightness contrast effect that has not been explained by other computer vision theories. In Fig. 9, although the luminances are equal at the left and right sides of the image within the dark frame, the filled-in output on the left half of the image is more intense ("brighter") than the output on the right. (Activation level is proportional to the size of the symbols at each location.) In Fig. 10, although the luminances are equal within the small square regions on the 135° diagonal in the upper-left and lower-right portions of the image, the filled-in output in the upper-left is more intense ("brighter") than the output on the lower-right. Both of the effects simulated in Figs. 9 and 10 correspond to brightness judgments of human observers.

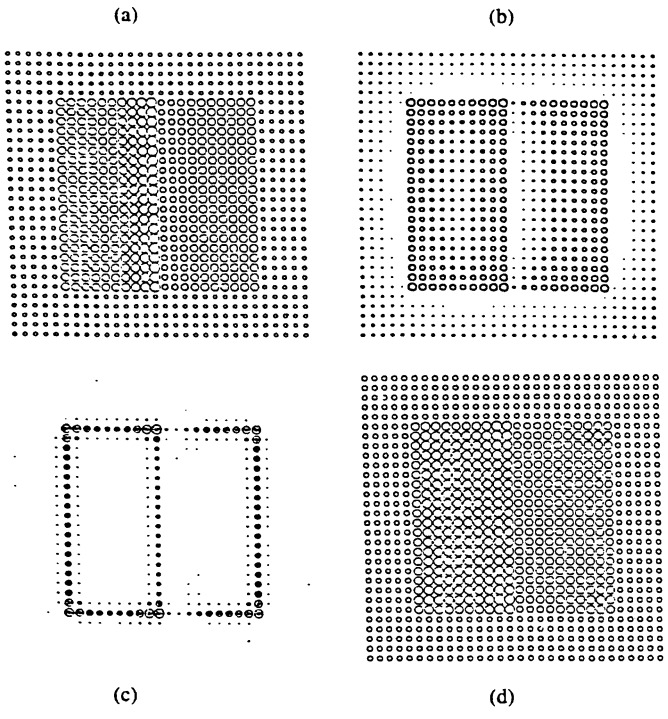

Fig. 9. Simulation of the Craik-O'Brien Cornsweet effect. The symbols of the units used in these simulations are introduced in Fig. 7. The size of the symbols codes the activity level of units at corresponding locations at different network levels. (a) The luminance distribution (stimulus). (b) The feature contour activity pattern that discounts the illuminant (feature). (c) The boundary segmentation (boundary). (d) The filled-in brightness profile (output).

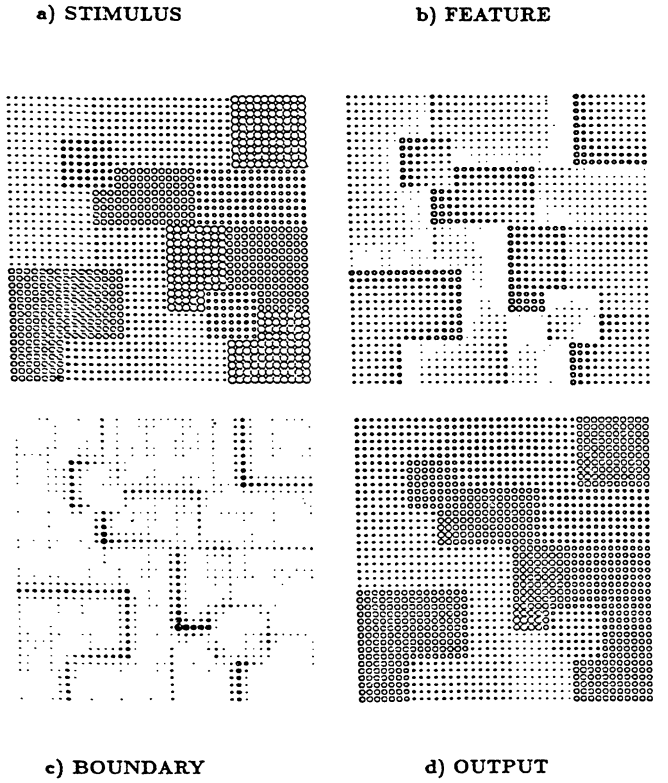

Fig. 10. Simulation of a Mondrian image. The depicted network levels are the same as in Fig. 7. See text for details.

In summary, the uncertainty of variable lighting conditions is resolved by discounting the illuminant and extracting contour-sensitive FC signals. The uncertainty created within the discounted regions is resolved at a later processing stage via a featural filling-in process that is activated by the FC signals and contained within boundaries defined by BC signals.

The Boundary Contour System and the Feature Contour System Obey Different Rules

Fig. 11 provides another type of evidence that feature contour and boundary contour information is extracted by separate, but parallel, neural subsystems before being integrated at a later stage into a unitary percept. By now, the total body of evidence for this new insight takes several forms: the two subsystems obey different rules; they can be used to explain a large body of perceptual data that has received no other unified explanation; they can be perceptually dissociated; when they are interpreted in terms of different neural substrates (the cytochrome-oxydase staining blob system and the hypercolumn system of the striate visual cortex and their prestriate cortical projections), their rules are consistent with known cortical data and have successfully predicted new cortical data [10], [12].

Fig. 11 illustrates several rule differences between the BCS and FCS. The reproduction process may have weakened the percept of an "illusory" square, which is called a Kanizsa square. The critical percept is that of the square's vertical boundaries. The black-gray vertical edge of the top-left pac-man figure is, relatively speaking, a dark-light vertical edge. The white-gray vertical edge of the bottom-left pac-man figure is, relatively speaking, a light-dark vertical edge. These two vertical edges possess the same orientation but opposite directions-of-contrast. The percept of the vertical boundary that spans these opposite direction-of-contrast edges shows that the BCS is sensitive to boundary orientation but is indifferent to direction-of-contrast. This observation is strengthened by the fact that the horizontal boundaries of the square, which connect edges of like direction-of-contrast, group together with the vertical boundaries to generate a unitary percept of a square. Opposite direction-of-contrast and same direction-of-contrast boundaries both input to the same BCS.

The FCS must, on the other hand, be exquisitely sensitive to direction-of-contrast. If FC signals were insensitive to direction-of-contrast, then it would be impossible to detect which side of a scenic edge possesses a larger reflectance, as in dark-light and red-green discriminations. Thus the rules obeyed by the two contour-extracting systems are not the same.

The BCS and the FCS differ in their spatial interaction rules in addition to their rules of contrast. For example, in Fig. 11, a vertical illusory boundary forms between the boundary contours generated by a pair of vertically-oriented and spatially aligned pac-man edges. Thus, the process of boundary completion is due to an *inwardly* di-

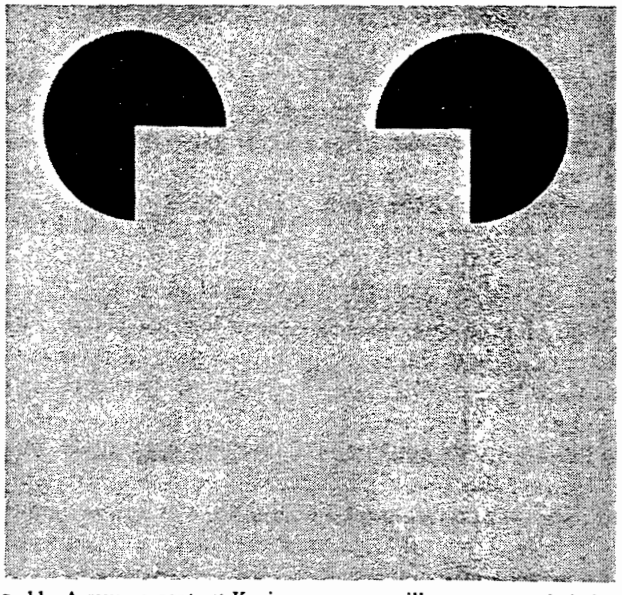

Fig. 11. A reverse-contrast Kanizsa square: an illusory square is induced by two black and two white pac-man figures on a grey background. Illusory contours can thus join edges with opposite directions-of-contrast. (This effect may be weakened by the photographic reproduction process.)

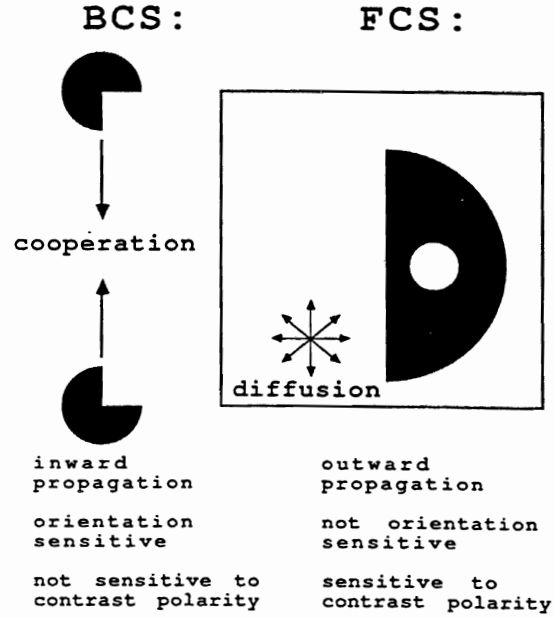

Fig. 12. Some computational differences between the BCS and FCS: the outcome of a BCS interaction is independent of direction-of-contrast, oriented and induced by pairs, or larger numbers, of oriented inducers. The outcome of an FCS interaction is dependent upon direction-of-contrast, unoriented, and generated by individual inducers.

rected and *oriented* interaction whereby *pairs* of inducing BC signals can trigger the formation of an intervening boundary of similar orientation. In contrast, in the filling-in reactions of Figs. 8–10, featural quality can flow from each FC signal in all directions until it hits a boundary contour or is attenuated by its own spatial spread. Thus featural filling-in is an *outwardly* directed and *unoriented* interaction that is triggered by *individual* FC signals. These differences between the BCS and FCS rules are summarized in Fig. 12.

Illusory Percepts as Probes of Adaptive Processes

The adaptive value of a featural filling-in process is clarified by considering how the nervous system discounts the illuminant. The adaptive value of a boundary completion process with properties capable of generating the percept of a Kanizsa square (Fig. 11) can be understood by considering other imperfections of the retinal uptake process. As noted above, light passes through retinal veins before it reaches retinal photoreceptors. Human observers do not perceive their retinal veins in part due to the action of mechanisms that attenuate the perception of images that are stabilized with respect to the retina.

Suppressing the perception of stabilized veins is insufficient, however, to generate an adequate percept. The images that reach the retina can be occluded and segmented by the veins in several places. Broken retinal contours need to be completed, and occluded retinal color and brightness signals need to be filled in. Holes in the retina, such as the blind spot or certain scotomas, are also not visually perceived due to a combination of boundary completion and filling-in processes. These completed boundaries and filled-in colors are illusory percepts, albeit illusory percepts with an important adaptive value. Observers are not aware which parts of such a completed figure are "real" (derived directly from retinal signals) or "illusory" (derived by boundary completion and featural filling-in). Thus, in a perceptual theory capable of understanding such completion phenomena, "real" and "illusory" percepts exist on an equal ontological footing. Consequently, we have been able to use the large literature on illusory figures, such as Figs. 1, 3, and 11, and filling-in reactions, such as in Figs. 8–10, to help us discover the distinct rules of BCS segmentation and FCS filling-in.

Boundary Contour Detection and Grouping Begins with Oriented Receptive Fields

Having distinguished the BCS from the FCS, the rules whereby boundaries are synthesized are now stated with increasing precision.

In order to effectively build up boundaries, the BCS must be able to determine the orientation of a boundary at every position. To accomplish this, the cells at the first stage of the BCS possess orientationally-tuned receptive fields, or oriented masks. Such a cell, or cell population, is selectively responsive to oriented contrasts that activate a prescribed small region of the retina, and whose orientations lie within a prescribed band of orientations with respect to the retina. A collection of such orientationally-tuned cells is assumed to exist at every network position, such that each cell type is sensitive to a different band of oriented contrasts within its prescribed small region of the scene, as in the hypercolumn model, which was developed to explain the responses of simple cells in area $V1$ of the striate cortex [17].

These oriented receptive fields illustrate that, from the very earliest stages of BCS processing, image contrasts

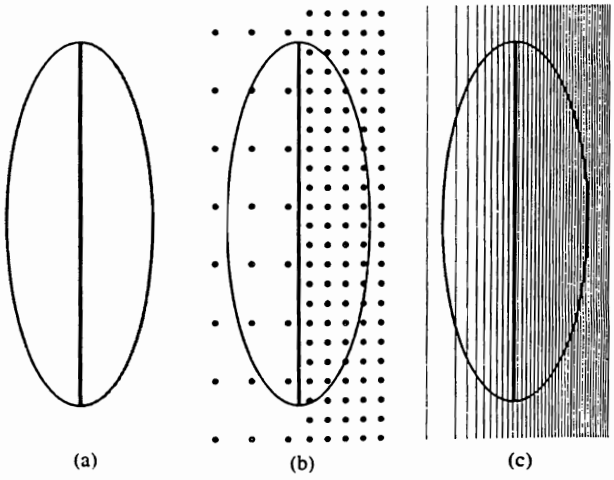

Fig. 13. Oriented masks respond to amount of luminance contrast over their elongated axis of symmetry, regardless of whether image contrasts are generated by (a) luminance step functions, (b) differences in textural distribution, or (c) smooth luminance gradients (indicated by the spacings of the lines).

are grouped and regrouped in order to generate configurations of ever greater global coherence and structural invariance. For example, even the oriented masks at the earliest stage of BCS processing regroup image contrasts. Such masks are oriented *local contrast* detectors, rather than edge detectors. This property enables them to fire in response to a wide variety of spatially nonuniform image contrasts that do not contain edges, as well as in response to edges (Fig. 13). In particular, such oriented masks can respond to spatially nonuniform densities of unoriented textural elements, such as dots. They can also respond to spatially nonuniform densities of surface gradients. Thus by sacrificing a certain amount of spatial resolution in order to detect oriented local contrasts, these masks achieve a general detection characteristic which can respond to boundaries, textures, and surfaces.

This general detection characteristic is achieved by using a relatively coarse weighted averaging and filtering of optical information at the earliest stages of the BCS. Such a coarse detection scheme obviates the need to proliferate a very large number of highly specialized detectors. In contrast, a vision system that postulated specialized dot, edge, angle, texture, shading, etc., detectors would be faced with a formidable problem of combining the data from each of these detectors. No less formidable is the problem that such specialized detectors often respond badly to other types of image statistics than the ones for which they are specialized. To overcome this problem, one would need an expert system to decide which type of detector should be applied to particular regions of a scene. Such a preprocessor would, however, have to solve the very problems that the vision system was supposed to solve. Thus, the reliance on highly specialized detectors leads to a formulation of the vision problem that does not work well on images whose properties are not narrowly defined, predictable, and controllable in advance.

On the other hand, the very properties of coarse sampling that lead to a general detection characteristic also imply a certain amount of informational uncertainty. From local estimates alone, such a detector cannot, for example, easily decide whether an edge, texture gradient, or shading gradient is present. The BCS thus accepts a certain amount of informational uncertainty at an early processing stage to ensure system versatility, and uses subsequent processing levels to help extract, sharpen, and complete from the spatial distribution of locally ambiguous signals those groupings which cohere into perceptually meaningful wholes.

In particular, the BCS is capable of automatically detecting and enhancing structures in a visual input by measuring inhomogeneities in the spatial distribution of local oriented contrasts against a statistical baseline that is determined by the input itself. This is done by a particular arrangement of short-range competition and long-range cooperation among orientation-sensitive nodes, following an initial stage of oriented-contrast filtering. Activations in groupings of nodes tuned to similar orientations that are approximately aligned in space receive a cooperative feedback advantage over randomly distributed network activations that arise from imaging noise. These random activations help to define the amount of aligned activity needed to be counted as signal. We now describe how this is done in greater detail.

An Uncertainty Principle: Orientational Certainty Implies Positional Uncertainty at Line Ends and Corners

The fact that the receptive fields of the BCS are *oriented* greatly reduces the number of possible groupings into which their target cells can enter. On the other hand, in order to detect oriented local contrasts, the receptive fields must be elongated along their preferred axis of symmetry. Then the cells can preferentially detect differences of average contrast across this axis of symmetry, yet can remain silent in response to differences of average contrast that are perpendicular to the axis of symmetry. Such receptive field elongation creates even greater positional uncertainty about the exact locations within the receptive field of the image contrasts which fire the cell. This positional uncertainty becomes acute during the processing of image line ends and corners.

Oriented receptive fields cannot easily detect the ends of thin scenic lines or scenic corners. This positional uncertainty is illustrated by the computer simulation in Fig. 14(a). The scenic image is a black vertical line (colored gray for illustrative purposes) against a white background. The line is drawn large to represent its scale relative to the receptive fields that it activates. In Fig. 14(a), each receptive field covers an area equivalent to 16×8 lattice points. The activation level of each oriented receptive field at a given position is proportional to the length of the line segment at that position which possesses the same orientation as the corresponding receptive field. The relative lengths of line segments across all positions encode the relative levels of receptive field activation due to different parts of the input pattern. We call such a spatial

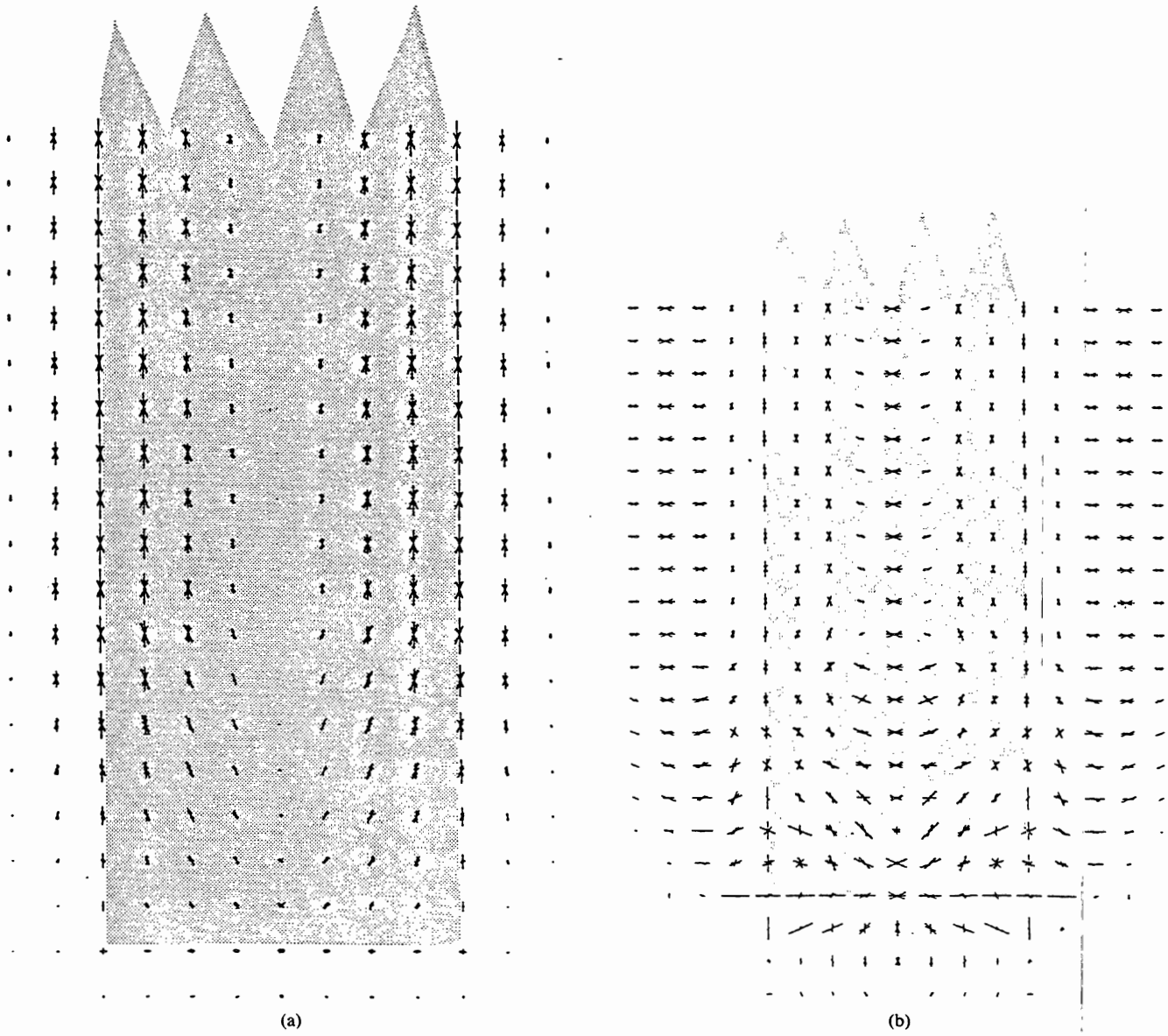

Fig. 14. (a) An orientation field: lengths and orientations of lines encode the relative sizes of the activations and orientations of the input masks at the corresponding positions. The input pattern, which is a vertical line end as seen by the receptive fields, correspond to the shaded area. Each mask has total exterior dimension of 16 × 8 units, with a unit length being the distance between two adjacent lattice positions. (b) Response of the second competitive stage, defined in (28) and Fig. 15, to the orientation field of Fig. 14(a): End cutting generates horizontal activations at line end locations that receive small and orientationally ambiguous input activations.

array of oriented responses an *orientation* field. An orientation field provides a concise statistical description in real-time of an image as seen by the receptive fields that it can activate. It models the responses of cortical simple cells in area $V1$ of the visual cortex [17].

In Fig. 14(a), a strong vertical reaction occurs at positions along the vertical sides of the input pattern that are sufficiently far from the bottom of the pattern. The contrast needed to activate these receptive fields was chosen low enough to allow cells with close-to-vertical orientations to be significantly activated at these positions. Despite the fact that cells were tuned to respond to relatively low contrasts, the cell responses at positions near the end of the line are very small. This result obtains in response to lines that are wider than lines which generate a continuous band of vertically-oriented responses throughout their interior, and are narrower than lines which generate a band of horizontally-oriented responses throughout their lowest extremity. Such a choice of lines always exist if the receptive field is elongated by a significant amount in a preferred orientation. Fig. 14(a) thus illustrates a basic uncertainty principle which says: orientational "cer-

tainty'' implies positional ''uncertainty'' at the ends of scenic lines whose widths are neither too small nor too large with respect to the dimensions of the oriented receptive field. The next section shows that a perceptual disaster would ensue in the absence of hierarchical compensation for this type of informational uncertainty.

Boundary-Feature Tradeoff: A New Organizational Principle

The perceptual disaster in question becomes clear when Fig. 14 is considered from the viewpoint of the featural filling-in process that compensates for discounting the illuminant, as in Figs. 8–10. If no BC signals are elicited at the ends of lines and at object corners, then in the absence of further processing within the BCS, boundary contours will not be synthesized to prevent featural quality from flowing out of all line ends and object corners within the FCS. Many percepts would hereby become badly degraded by featural flow.

Thus, basic constraints upon visual processing seem to be seriously at odds with each other. The need to discount the illuminant leads to the need for featural filling-in. The need for featural filling-in leads to the need to synthesize boundaries capable of restricting featural filling-in to appropriate perceptual domains. The need to synthesize boundaries leads to the need for orientation-sensitive receptive fields. Such receptive fields are, however, unable to restrict featural filling-in at scenic line ends or sharp corners. Thus, orientational certainty implies a type of positional uncertainty, which is unacceptable from the perspective of featural filling-in requirements. Indeed, an adequate understanding of how to resolve this uncertainty principle is not possible without considering featural filling-in requirements. That is why perceptual theories which have not clearly distinguished the complementary computational requirements of the BCS and FCS have not adequately characterized how perceptual boundaries are formed. We call the complementary design balance that exists between BCS and FCS design requirements the *boundary-feature tradeoff*.

We now summarize how later stages of BC system processing compensate for the positional uncertainty that is created by the orientational tuning of receptive fields.

The Hierarchical Resolution of Orientation-Induced Uncertainty: All Line Ends are Illusory

Fig. 14(b) depicts the reaction of the BC system's next processing stages to the input pattern depicted in Fig. 14(a). Strong horizontal activations are generated at the end of the scenic line by these processing stages. These horizontal activations are capable of generating a horizontal boundary within the BCS whose output signals, as in Figs. 4 and 7, prevent flow of featural quality from the end of the line within the FCS. These horizontal activations form an ''illusory'' boundary, in the sense that this boundary is not directly extracted from luminance differences in the scenic image. The theory hereby suggests that the perceived ends of all such thin lines are generated by such ''illusory'' line end inductions, which we call *end cuts*. This conclusion is sufficiently remarkable to summarize it with a maxim: *all line ends are illusory*.

This seemingly paradoxical maxim can be understood as one manifestation of how the visual system overcomes, using multiple processing stages, the informational uncertainties that it cannot overcome at a single processing stage. In the present example, orientational tuning of receptive fields is needed to partially overcome the uncertainty of an image edge's orientation but in so doing renders uncertain the positions of the ends and corners of such edges. Later processing stages are needed to recover both the positional and orientational data that are lost in this way.

The OC Filter and the Short-Range Competitive Stages

The processing stages that are hypothesized to generate end cuts are summarized in Fig. 15. First, oriented-receptive fields of like position and orientation, but opposite direction-of-contrast, generate rectified output signals that summate at the next processing stage to activate cells whose receptive fields are sensitive to the same position and orientation as themselves, but are insensitive to direction-of-contrast. These target cells maintain their sensitivity to *amount* of oriented contrast, but not to the *direction* of this oriented contrast, as in our explanation of Fig. 12. Such model cells, which play the role of complex cells in area $V1$ of the visual cortex, pool inputs from receptive fields with opposite directions-of-contrast, which play the role of simple cells in area $V1$, in order to generate boundary detectors which can detect the broadest possible range of luminance or chromatic contrasts [7], [24]. These two successive stages of oriented contrast-sensitive cells are called the OC filter. Equations (8)–(16) above model simple cells and complex cells in our computer simulations of invariant brightness perception.

The rectified output from the OC filter activates a second filter which is composed of two successive stages of spatially short-range competitive interaction whose net effect is to generate end cuts (Fig. 15). First, a cell of prescribed orientation excites like-oriented cells corresponding to its location and inhibits like-oriented cells corresponding to nearby locations at the next processing stage. In other words, an on-center off-surround organization of like-oriented cell interactions exists around each perceptual location. This mechanism is analogous to the neurophysiological process of *end stopping*, whereby hypercomplex cell receptive fields are fashioned from interactions of complex cell output signals [16], [21]. The outputs from this competitive mechanism interact with the second competitive mechanism. Here, cells compete that represent different orientations, notably perpendicular orientations, at the same perceptual location. This competition defines a push–pull opponent process. If a given orientation is excited, then its perpendicular orientation is

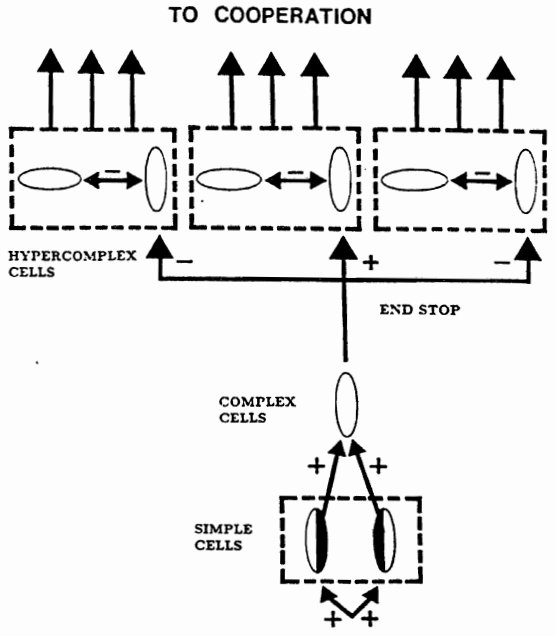

Fig. 15. Early stages of boundary contour processing: at each position exist cells with elongated receptive fields (simple cells) of various sizes which are sensitive to orientation, amount-of-contrast, and direction-of-contrast. Pairs of such cells sensitive to like orientation but opposite directions-of-contrast (lower dashed box) input to cells (complex cells) that are sensitive to orientation and amount-of-contrast but not to direction-of-contrast (white ellipses). These cells, in turn, excite like-oriented cells (hypercomplex cells) corresponding to the same position and inhibit like-oriented cells corresponding to nearby positions at the first competitive stage. At the second competitive stage, cells corresponding to the same position but different orientations (higher-order hypercomplex cells) inhibit each other via a push–pull competitive interaction.

inhibited. If a given orientation is inhibited, then its perpendicular orientation is excited via disinhibition.

The combined effect of these two competitive interactions generate end cuts as follows. The strong vertical activations along the edges of a scenic line, as in Fig. 14(a), inhibit the weak vertical activations near the line end. These inhibited vertical activations, in turn, disinhibit horizontal activations near the line end, as in Fig. 14(b). Thus, the positional uncertainty generated by orientational certainty is eliminated at a subsequent processing level by the interaction of two spatially short-range competitive mechanisms which convert complex cells into two distinct populations of hypercomplex cells.

The properties of these competitive mechanisms have successfully predicted and helped to explain a variety of neural and perceptual data. For example, the prediction of the theory summarized in Fig. 14 predated the report by von der Heydt, Baumgartner, and Peterhans [27] that cells in prestriate visual cortex respond to perpendicular line ends, as in Fig. 14(b), whereas cells in striate visual cortex do not, as in Fig. 14(a). These cells properties also help to explain why color is sometimes perceived to spread across a scene, as in the phenomenon of neon color spreading [10], [12], [22], by showing how some BC signals are inhibited by boundary contour processes. An example of neon color spreading can be found on the cover of the journal *neural networks* where it is placed to emphasize how an emergent behavioral property can be induced by form-color interactions triggered across a whole scene. In that example, the red crosses in the image form the crosses of a cross-bar associative network. Such competitive interactions also clarify many properties of perceptual grouping, notably of the "emergent features" that group textures into figure and ground [1], [11], [12]. Such percepts can be explained by the end cutting mechanism when it interacts with the next processing stage of the BCS.

Long-Range Cooperation: Boundary Completion and Emergent Features

The outputs from the competition input to a spatially long-range cooperative process, called the *boundary completion* process. This cooperative process helps to build up sharp coherent global boundaries and emergent segmentations from noisy local boundary fragments. In the first stage of this boundary completion process, outputs from the second competitive stage from (approximately) like-oriented cells that are (approximately) aligned across perceptual space cooperate to begin the synthesis of an intervening boundary. For example, such a boundary completion process can span the blind spot and the faded stabilized images of retinal veins. The same boundary completion process is used to complete the sides of the Kanizsa square in Fig. 12. Further details about this boundary completion process can be derived once it is understood that the boundary completion process overcomes a different type of informational uncertainty than is depicted in Fig. 14.

This type of uncertainty is clarified by considering Fig. 16. The percept in Fig. 16(a), as well as those in Figs. 3 and 16(b), can be understood as a byproduct of four processes: within the BCS, perpendicular end cuts at the line ends [Fig. 14(b)] cooperate to complete a emergent boundary which separates the visual field into two domains. This completed boundary structure sends topographically organized boundary signals into the FCS (Fig. 7), thereby dividing the FCS into two domains. If different filling-in contrasts are induced within these domains due to the FC signals generated by the black scenic lines, then the illusory figure can become visible.

Fig. 16(a) shows that the tendency to form boundaries that are perpendicular to line ends is a strong one; the completed boundary forms sharp corners to keep the boundary perpendicular to the inducing scenic line ends. Fig. 16(b) shows, however, that the boundary completion process can generate a boundary that is not perpendicular to the inducing line ends under certain circumstances.

Orientational Uncertainty and the Initiation of Boundary Completion

A comparison of Fig. 16(a) and (b) indicates the nature of the third problem of uncertain measurement that we have encountered. Fig. 16(a) and (b) show that boundary completion can occur within *bands* of orientations, which describe a type of real-time local probability distribution

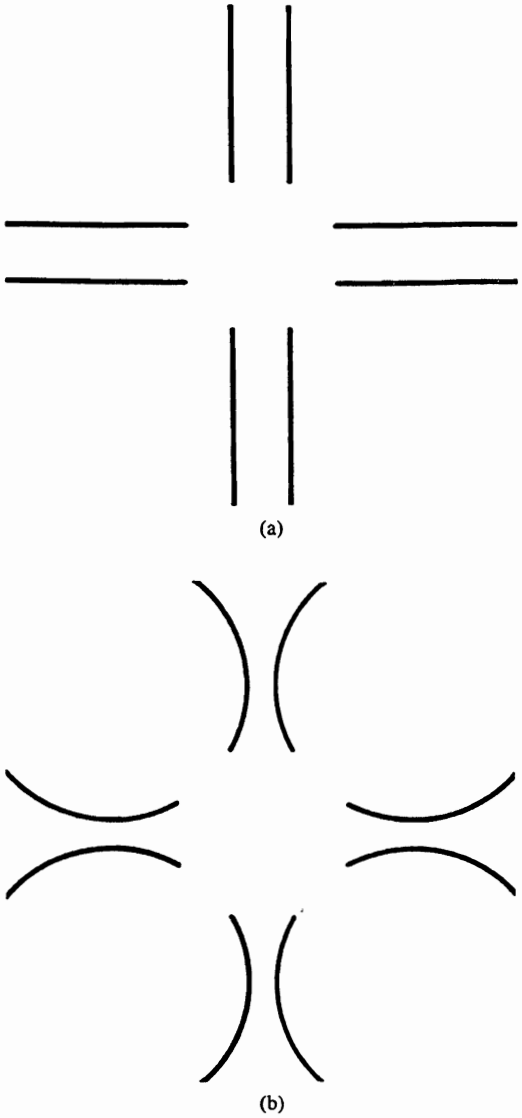

Fig. 16. (a) An illusory square forms perpendicular to all line ends. The global grouping confirms all the locally preferred perpendicular grouping orientations. (b) An illusory square forms almost perpendicular to all line ends. The global grouping amplifies grouping orientations that are not locally preferred and competitively inhibits the locally preferred perpendicular orientations. Both emergent segmentations (a) and (b) are sharp despite the fact that fuzzy bands of possible grouping orientations must exist.

for the orientations in which grouping can be initiated at each position. These orientations include the orientations that are perpendicular to their inducing line ends [Fig. 16(a)], as well as nearby orientations that are not perpendicular to their inducing line ends [Fig. 16(b)]. Fig. 14(b) illustrates how such a band of end cuts can be induced at the end of a scenic line. The existence of such bands of possible orientations increases the probability that spatially separated boundary segments can begin to group cooperatively into a global boundary. If only a single orientation at each spatial location were activated, then the probability that these orientations could precisely line up across perceptual space to initiate boundary completion would be vanishingly small. The (partial) orientational uncertainty that is caused by bands of orientations is thus a useful property for the initiation of the perceptual grouping process that controls boundary completion and textural segmentation.

Such orientational uncertainty can, however, cause a serious loss of acuity in the absence of compensatory processes. If *all* orientations in each band could cooperate with *all* approximately aligned orientations in nearby bands, then a fuzzy band of completed boundaries, rather than a single sharp boundary, could be generated. The existence of such fuzzy boundaries would severely impair visual clarity. Fig. 16 illustrates that only a single sharp boundary usually becomes visible despite the existence of oriented bands of boundary inducers. How does the nervous system resolve the uncertainty produced by the existence of orientational bands? How is a single global boundary chosen from among the many possible boundaries that fall within the local oriented bandwidths?

Our answer to these questions suggests a basic reason why later stages of boundary contour processing must send nonlinear feedback signals to earlier stages of boundary contour processing. This cooperative feedback provides a particular grouping of orientations with a competitive advantage over other possible groupings by exploiting the competitive interactions described above.

Boundary Completion by Cooperative–Competitive Feedback Networks: The CC Loop

We assume, as is illustrated by Fig. 11, that pairs of similarly oriented and spatially aligned cells of the second competitive stage are needed to activate the intervening cooperative cells that subserve boundary completion (Fig. 17). These cells, in turn, feed back excitatory signals to like-oriented cells at the first competitive stage, which feeds into the competition between orientations at each position of the second competitive stage. Thus, in Fig. 16, positive feedback signals are triggered in pathway 2 by a cooperative cell if sufficient activation simultaneously occurs in both of the feedforward pathways labeled 1 from similarly oriented cells of the second competitive stage. Then both pathways labeled 3 can trigger feedback in pathway 4. This feedback exchange can rapidly complete an oriented boundary between pairs of inducing scenic contrasts via a spatially discontinuous bisection process.

Such a boundary completion process realizes a new type of real-time statistical decision theory. Each cooperative cell is sensitive to the position, orientation, density, and size of the inputs that it receives from the second competitive stage. Each cooperative cell performs like a type of statistical "and" gate since it can only fire feedback signals to the first competitive stage if both of its branches are sufficiently activated. We call such cooperative cells *bipole* cells. The existence of such bipole cells was predicted by our theory. Von der Heydt, Baumgartner, and Peterhans [27] reported the existence of such cells in the prestriate visual cortex, in the same report that confirmed the existence of prestriate cells which respond to perpen-

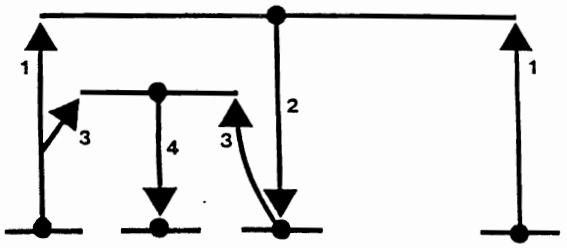

Fig. 17. A cooperative-competitive feedback exchange leading to boundary completion: cells at the bottom row represent like-oriented cells at the second competitive stage whose orientational preferences are approximately aligned across perceptual space. The cells in the top two rows are bipole cells in the cooperative layer whose receptive field pairs are oriented along the axis of the competitive cells. Suppose that simultaneous activation of the pair of pathways 1 activates positive boundary completion feedback along pathway 2. Then pairs of pathways such as 3 activate positive feedback along pathways such as 4. Rapid completion of a sharp boundary between the locations of pathways 1 can hereby be generated by a spatially discontinuous bisection process.

dicular line ends, as in Fig. 14(b). See [10] for a summary of these and related neurophysiological data. The entire cooperative-competitive feedback network is called the CC loop.

Equations for a Monocular Version of the Boundary Contour System

Fig. 18 depicts a BCS circuit that combines the OC filter and the CC loop. The following neural network equations represent a monocular, single-scale version of the OC filter and the CC loop. All processes, except the first competitive stage, are assumed to react so quickly that they can be represented at equilibrium as algebraic equations. This approximation speeds up the simulations, but does not influence the results. See Grossberg and Mingolla [13] for more complete definitions of these network processes. See Grossberg and Mingolla [14] for a modified version of this system.

As in (1)–(22), indexes (i, j) represent a cell position within a two-dimensional lattice and k represents an orientation.

OC Filter

Oriented Filter: Complex Cell Receptive Fields

For simplicity, a different simple cell and complex cell model was used than in (8)–(16). Many variants are possible, including models based upon Gabor filters.

Letting X_{pq} equal the input to position (p, q),

$$J_{ijk} = \frac{[U_{ijk} - \alpha V_{ijk}]^+ + [V_{ijk} - \alpha U_{ijk}]^+}{1 + \beta(U_{ijk} + V_{ijk})} \tag{23}$$

where

$$U_{ijk} = \sum_{(p,q)\in L_{ijk}} X_{pq} \tag{24}$$

$$V_{ijk} = \sum_{(p,q)\in R_{ijk}} X_{pq} \tag{25}$$

and the notation $[p]^+ = \max(p, 0)$. In (23), the elongated receptive field is divided into a left-half L_{ijk} and a right-half R_{ijk}. The simple cell terms $U_{ijk} - \alpha V_{ijk}$ could be replaced by a Gabor filter, or a related oriented filter.

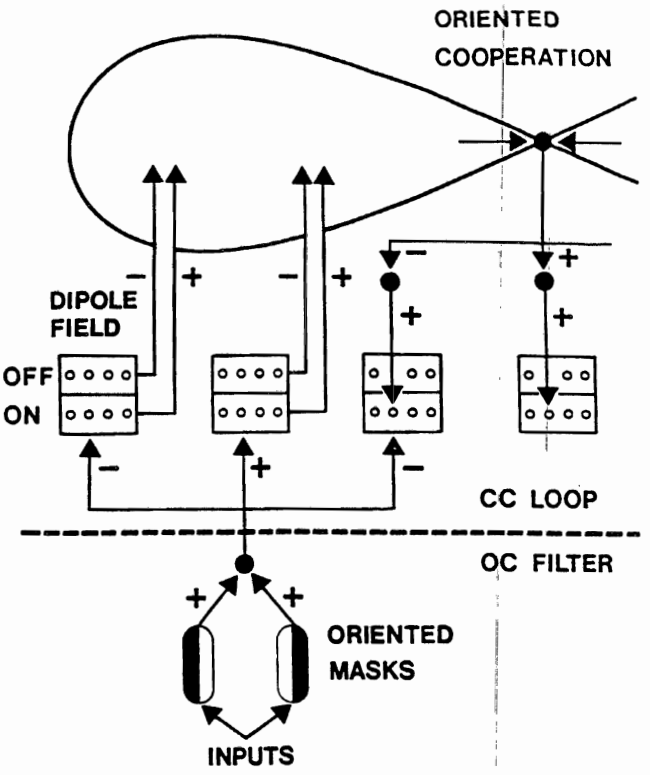

Fig. 18. Circuit diagram of the OC filter and CC loop of the BCS: the OC filter contains the simple cell and complex cell filter shown in Fig. 15. The CC loop contains the first and second competitive stages shown in Fig. 15, as well as the feedback interaction of these competitive stages with the cooperative bipole cells shown in Fig. 17. Additional BCS features are also here summarized: the hypercomplex cells of Fig. 15 are the on-cells of a dipole field. As in Fig. 15, on-cells at a fixed position compete among orientations. On-cells also inhibit off-cells which represent the same position and orientation. Off-cells at each position, in turn, compete among orientations. Both on-cells and off-cells are tonically active. As in Fig. 17, net excitation of an on-cell excites a similarly oriented cooperative bipole cell at a location corresponding to that of the on-cell. In addition, net excitation of an off-cell inhibits a similarly oriented cooperative bipole cell at a location corresponding to that of the off-cell. Thus, bottom-up excitation of a vertical on-cell, by inhibiting on-cell at that position, disinhibits the horizontal off-cell at that position, which in turn inhibits (almost) horizontally oriented cooperative bipole cells whose receptive fields include its position. Sufficiently strong net positive activation of both receptive fields of a cooperative bipole cell enables it to generate feedback via an on-center off-surround interaction among the like-oriented cells. On-cells which receive the most favorable combination of bottom-up signals and top-down signals generate the emergent perceptual grouping.

CC Loop

First Competitive Stage: Hypercomplex Cells

$$\frac{d}{dt} w_{ijk} = -w_{ijk} + I + BJ_{ijk} + v_{ijk} - B \sum_{(p,q)} J_{pqk} A_{pqij}. \tag{26}$$

Second Competitive Stage: Higher-Order Hypercomplex Cells

$$O_{ijk} = C[w_{ijk} - w_{ijK}]^+ \tag{27}$$

$$y_{ijk} = \frac{EO_{ijk}}{D + O_{ij}} \tag{28}$$

where K is the orientation perpendicular to k, and $O_{ij} = \Sigma_{k=1}^{n} O_{ijk}$.

Cooperation: Oriented And-Gates

$$z_{ijk} = g\left(\sum_{(p,q,r)} [y_{pqr} - y_{pqR}] F_{pqij}^{(r,k)}\right) + g\left(\sum_{(p,q,r)} [y_{pqr} - y_{pqR}] G_{pqij}^{(r,k)}\right) \tag{29}$$

where

$$g(s) = \frac{H[s]^+}{K + [s]^+} \tag{30}$$

and kernels $F_{pqij}^{(r,k)}$ and $G_{pqij}^{(r,k)}$ define the cell's two oriented receptive fields.

Cooperative Feedback to First Competitive Stage

$$v_{ijk} = \frac{h(z_{ijk})}{1 + \sum_{(p,q)} h(z_{pqk}) W_{pqij}} \tag{31}$$

where

$$h(s) = L[s - M]^+. \tag{32}$$

When a complete BCS is used to regulate the filling-in process described in (1)–(22), then the variables Z_{ijk} in (18) are replaced by y_{ijk} in (28).

The CC loop can generate a sharp emergent boundary from a fuzzy band of possible boundaries for the following reason. As in Fig. 16, certain orientations at given position are more strongly activated than other orientations. Suppose that the cells which encode a particular orientation at two or more approximately aligned positions can more strongly activate their target bipole cells than can the cells which encode other orientations. Then competitive cells of similar orientation at intervening positions will receive more intense excitatory feedback from these bipole cells. This excitatory feedback enhances the activation of these competitive cells relative to the activation of cells which encode other orientations. This advantage enables the favored orientation to suppress alternative orientations due to the orientational competition that occurs at the second competitive stage (Fig. 15).

A preattentive BCS representation emerges when CC loop dynamics approach a nonzero equilibrium activity pattern. The nonlinear feedback process whereby an emergent line or curve is synthesized need not even define a connected set of activated cells until equilibrium is approached. This process sequentially interpolates boundary components within progressively finer spatial intervals until a connected configuration is attained. Thus, *continuous boundaries are completed discontinuously.*

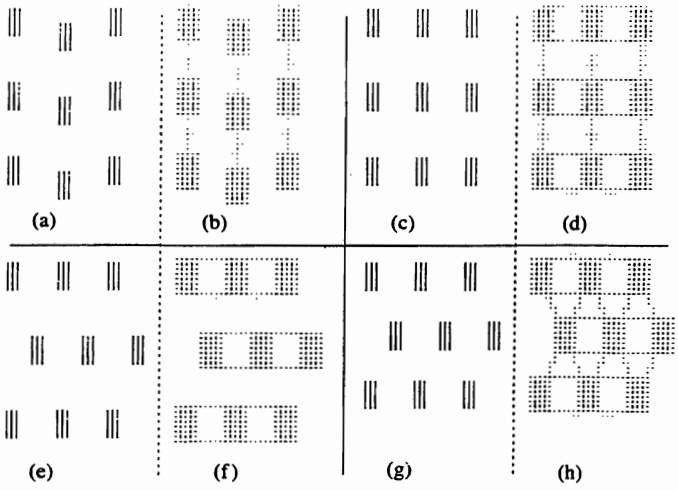

Fig. 19. Computer simulations of processes underlying textural grouping. The length of each line segment is proportional to the activation of a network node responsive to one of twelve possible orientations. Parts (a), (c), (e), and (g) display the activities of oriented cells which input to the CC loop. Parts (b), (d) (f), and (h) display equilibrium activities of oriented cells at the second competitive stage of the CC loop. A pairwise comparison of (a) with (b), (c) with (d), and so on indicates the major groupings sensed by the network. These simulations demonstrate that an emergent segmentation can form colinear to—as in (b) and (d),—perpendicular to—as in (d), (f), and (h), or diagonal to—as in (h), the inducing vertically oriented Lines by merely changing the relative positions of these lines. See text for details.

Textural Grouping

Fig. 19 depicts the results of computer simulations which illustrate how these properties of the CC loop can generate a perceptual grouping or emergent segmentation of figural elements (as in Fig. 2). Fig. 19(a) depicts an array of nine vertically-oriented input clusters. Each cluster is called a Line because it represents a caricature of how a field of OC filter output cells respond to a vertical line. Fig. 19(b) displays the equilibrium activities of the cells at the second competitive stage of the CC loop in response to these Lines. The length of an oriented Line at each position is proportional to the equilibrium activity of a cell whose receptive field is centered at that position with that orientation. The input pattern in Fig. 19(a) possesses a vertical symmetry: triples of vertical Lines are colinear in the vertical direction, whereas they are spatially out-of-phase in the horizontal direction. The BCS senses this vertical symmetry, and generates emergent vertical boundaries in Fig. 19(b). The BCS also generates horizontal end cuts at the ends of each Line, which can trap the featural contrasts of each Line within the FCS. Thus, the emergent segmentation simultaneously supports a vertical macrostructure and a horizontal microstructure among the Lines.

In Fig. 19(c), the input Lines are moved so that triples of Lines are colinear in the vertical direction and their Line ends are lined up in the horizontal direction. Both vertical and horizontal boundary groupings are generated in Fig. 19(d). The segmentation distinguishes between Line ends and the small horizontal inductions that bound the sides of each Line. Only Line ends have enough sta-

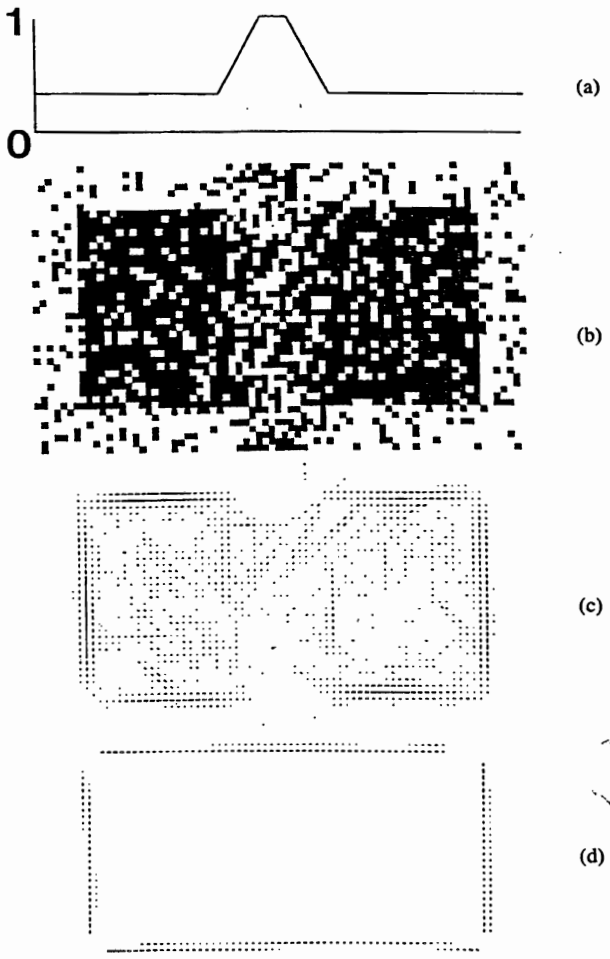

Fig. 20. (a) Distribution of noise in horizontal dimension of image; (b) binary image of a rectangle corrupted by noise whose distribution, as in (a), varies continuously; (c) responses of oriented contrast detectors to the image; (d) equilibrated responses of cooperative feedback cells of BC system. The rectangle is recovered and the ramped increase of noise in the middle of the figure is ignored.

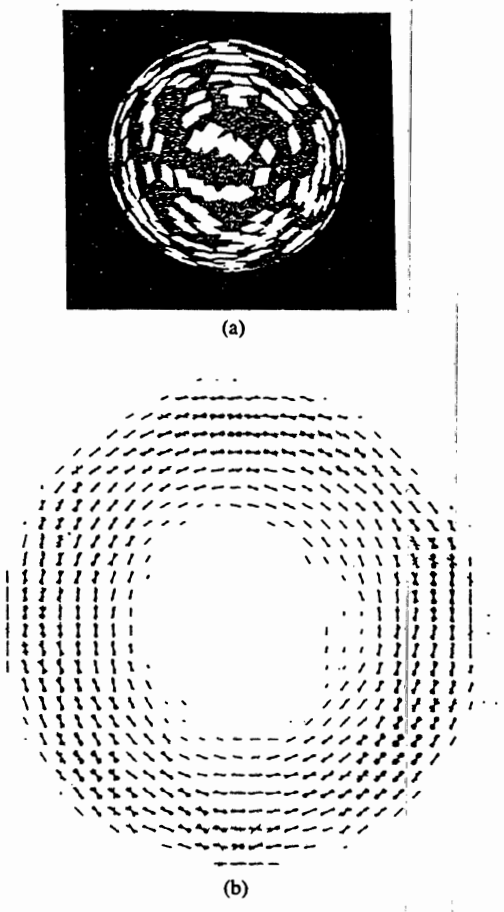

Fig. 21. (a) A textured, curved surface (adapted from [25]). (b) Equilibrated response of cooperative feedback cells of the CC loop to the inputs from Fig. 21(a). The cooperative cells group the circular statistics of the parallelogram orientations near the figure's periphery, but suppress the discordant orientations near the center. A similar grouping process generates the circular segmentations induced by the Glass pattern in Fig. 1.

tistical inertia to activate horizontal boundary completion via the CC loop.

In Fig. 19(e), the input Lines are shifted to that they become noncolinear in a vertical direction, but triples of their Line ends remain aligned. The vertical symmetry of Fig. 19(c) is hereby broken. Consequently, in Fig. 19(f) the BCS groups the horizontal Line ends, but not the vertical Lines.

Fig. 19(h) depicts the emergence of diagonal groupings where no diagonals exist in the input pattern. Fig. 19(g) is generated by bringing the three horizontal rows of vertical Lines close together until their ends lie within the spatial bandwidth of the cooperative interaction. In Fig. 19(h), the BCS senses diagonal groupings of the Lines. Diagonally-oriented receptive fields are activated in the emergent boundaries, and these activations, as a whole, group into diagonal bands. Thus, these diagonal groupings emerge on both microscopic and macroscopic scales. The computer simulations illustrated in Fig. 19 show that the CC loop can generate large-scale segmentations without a loss of positional or orientational acuity.

The computer simulations of textural grouping in Fig. 19 do not deny that the two successive filters defined by the OC filter and the short-range competitive stages (Fig. 15) contribute to percepts of texture. Beck, Sutter, and Ivry [2] have provided recent experimental evidence supporting the role of these filters in texture segregation.

A number of other important properties of emergent segmentation have also been demonstrated through computer simulations of the BCS. Fig. 20 illustrates the BCS's ability to detect and complete sharp boundaries over long distances in the presence of severe noise, a type of capability useful in penetrating camouflage. This simulation illustrates the response of spatial scale large enough to group across individual image contrasts. Smaller spatial scales generate the boundaries of individual black and white compartments.

Fig. 21 illustrates the BCS's ability to detect form within a 2-D texture. Although the input is a pattern of discrete texture elements [Fig. 21(a)] the BCS can generate a dense *boundary web* of form-sensitive emergent groupings [Fig. 21(b)]. In a multiple scale version of the BCS, these boundary webs help to explain the percept of

a smoothly curved 3-D surface. Todd and Akerstrom [25] have shown that the worst correlation between human psychophysical judgments of 3-D shape-from-texture and the theoretical predictions of such a multiple scale version of the BCS was 0.985. Meyer and Dougherty [20] have further shown that the theory is consistent with data about the effects of flicker-induced depth on chromatic subjective contours. The theory has also been able to analyze and predict many other perceptual and neural data that other vision theories cannot yet handle.

Thus, although a great deal of work remains to be done on further development of the BCS, the FCS, and their interactions, many promising results suggest that we are well along the way towards a better understanding of biologically-motivated vision systems which are equally at home in segmenting and filling-in the full range of visual phenomena—boundaries, textures, surfaces—from the discrete to the continuous.

REFERENCES

[1] J. Beck, K. Prazdny, and A. Rosenfeld, "A theory of textural segmentation," in, *Human and Machine Vision*, J. Beck, B. Hope, and A. Rosenfeld, Eds. New York: Academic, 1983.

[2] J. Beck, A. Sutter, and R. Ivry, "Spatial frequency channels and perceptual grouping in texture segregation," Preprint, 1987.

[3] G. A. Carpenter and S. Grossberg, "A massively parallel architecture for a self-organizing neural pattern recognition machine," *Comput. Vis., Graph., Image Proc.*, vol. 37, pp. 54–115, 1987.

[4] ——, "ART 2: Stable self-organization of pattern recognition codes for analog input patterns," *Appl. Opt.*, vol. 26, pp. 4919–4930, 1987.

[5] ——, "The ART of adaptive pattern recognition by a self-organizing neural network," *Computer*, vol. 21, pp. 77–88, 1988.

[6] M. A. Cohen and S. Grossberg, "Neural dynamics of brightness perception: Features, boundaries, diffusion, and resonance," *Percep. Psychophys.*, vol. 36, pp. 428–456, 1984.

[7] R. L. DeValois, D. G. Albrecht, and L. G. Thorell, "Spatial frequency selectivity of cells in macaque visual cortex," *Vision Res.*, vol. 22, pp. 545–559, 1982.

[8] S. Geman and D. Geman, "Stochastic relaxation, Gibbs distribution, and the Bayesian restoration of images," *IEEE Pattern Anal. Mach. Intell.*, vol. PAMI-6, pp. 721–741, 1984.

[9] S. Grossberg, "The quantized geometry of visual space: The coherent computation of depth, form, and lightness," *Behavioral Brain Sci.*, vol. 6, pp. 625–657, 1983.

[10] ——, "Cortical dynamics of three-dimensional form, color, and brightness perception, I: Monocular theory," *Percep. Psychophys.*, vol. 41, pp. 87–116, 1987.

[11] ——, "Cortical dynamics of three-dimensional form, color, and brightness perception, II: Binocular theory," *Percep. Psychophys.*, vol. 41, pp. 117–158, 1987.

[12] S. Grossberg and E. Mingolla, "Neural dynamics of form perception: Boundary completion, illusory figures, and neon color spreading," *Psychol. Rev.*, vol. 92, pp. 173–211, 1985.

[13] ——, "Neural dynamics of perceptual grouping: Textures, boundaries, and emergent segmentations," *Percep. Psychophys.*, vol. 38, pp. 141–171, 1985.

[14] ——, "Neural dynamics of surface perception: Boundary webs, illuminants, and shape-from-shading," *Comput. Vis., Graph., Image Proc.*, vol. 37, pp. 116–165, 1987.

[15] S. Grossberg and D. Todorović, "Neural dynamics of 1-D and 2-D brightness perception: A unified model of classical and recent phenomena," *Percep. Psychophys.*, vol. 43, pp. 241–277, 1988.

[16] D. H. Hubel and T. N. Wiesel, "Receptive fields and functional architecture in two nonstriate visual areas (18 and 19) of the cat," *J. Neurophysiol.*, vol. 28, pp. 229–289, 1965.

[17] ——, "Functional architecture of macaque monkey visual cortex," *Proc. Roy. Soc. London B*, vol. 198, pp. 1–59, 1977.

[18] S. Kirkpatrick, D. D. Gelatt, and M. P. Vecchi, "Optimization by simulated annealing," *Science*, vol. 220, pp. 671–680, 1983.

[19] E. H. Land, "The retinex theory of color vision," *Sci. Amer.*, vol. 237, pp. 108–128, 1977.

[20] G. E. Meyer and T. Dougherty, "Effects of flicker-induced depth on chromatic subjective contours," *J. Exp. Psych.: Human Percep. Perform.*, vol. 13, pp. 353–360, 1987.

[21] G. A. Orban, H. Kato, and P. O. Bishop, "Dimensions and properties of end-zone inhibitory areas in receptive fields of hypercomplex cells in cat striate cortex," *J. Neurophysiol.*, vol. 42, pp. 833–849, 1979.

[22] C. Redies and L. Spillmann, "The neon color effect in the Ehrenstein illusion," *Perception*, vol. 10, pp. 667–681, 1981.

[23] E. L. Schwartz, R. Desimone, T. Albright, and C. Gross, "Shape recognition and inferior temporal neurons," *Proc. Nat. Acad. Sci.*, vol. 80, pp. 5776–5778, 1983.

[24] H. Spitzer and S. Hochstein, "A complex-cell receptive field model," *J. Neurophysiol.*, vol. 53, pp. 1266–1286, 1985.

[25] J. T. Todd and R. A. Akerstrom, "Perception of three-dimensional form from patterns of optical texture," *J. Exp. Psych.: Human Percep. Perform.*, vol. 13, pp. 242–255, 1987.

[26] A. Treisman and H. Schmidt, "Illusory conjunctions in the perception of objects," *Cognitive Psych.*, vol. 14, pp. 107–141, 1982.

[27] R. von der Heydt, E. Peterhaus, and G. Baumgartner, "Illusory contours and cortical neuron responses," *Science*, vol. 224, pp. 1260–1262, 1984.

[28] A. L. Yarbus, *Eye Movements and Vision*. New York: Plenum, 1967.

Stephen Grossberg received graduate training at Stanford University, Stanford, CA, and Rockefeller University.

He was a Professor at Massachusetts Institute of Technology, Cambridge, MA. Currently, he is a Professor of Mathematics, Psychology, and Biomedical Engineering at Boston University, Boston, MA, where he founded and is the Director of the Center for Adaptive Systems, and Director of the University's new graduate program in Cognitive and Neural Systems. During the past few decades, he and his colleagues at the Center for Adaptive Systems have pioneered and developed a number of the fundamental principles, mechanisms, and architectures that form the foundation for contemporary neural network research. These investigations include contributions to biological vision and multidimensional image processing; cognitive information processing; adaptive pattern recognition; speech and language perception, learning, and production; adaptive robotics; conditioning and attention; development; biological rhythms; certain mental disorders; and their substrates in neurophysiological and anatomical mechanisms. A hallmark of this work is its focus upon the design principles and mechanisms which enable the behavior of individuals to adapt successfully in real time to unexpected environmental changes. The core models pioneered by this approach and which are embedded in these neural network theories include models which go under such names as competitive learning, adaptive resonance theory, masking fields, gated dipole opponent processes, associative outstars and instars, associative avalanches, associative spatial maps, nonlinear cooperative-competitive feedback networks, boundary contour and feature contour systems, adaptive vector encoders, and vector integration to endpoint circuits. Such models have been used both the analyze and predict a wide range of interdisciplinary data about mind and brain, as well as to suggest novel architectures for technological applications.

Prof. Grossberg is Founder and First President of the International Neural Network Society and a coeditor-in-chief of the Society's journal *Neural Networks*.

Ennio Mingolla was an undergraduate philosophy major at Harvard College, Cambridge, MA, before teaching secondary school science and mathematics in Liberia as a Peace Corps volunteer. While working as an analyst in applied social science research at Abt Associates of Cambridge, Massachusetts, he received the M.Ed degree at Boston University, Boston, MA, in educational media.

His doctoral training in experimental psychology at the University of Connecticut, Storrs, involved a concentration in human visual perception and a secondary concentration in computer science. His dissertation research involved using computer graphics displays for stimulus generation for the first parametric studies of human perception of shape-from-shading, in which many of the assumptions of existing computational approaches to shape-from-shading were found to be at odds with human performance. Since receiving his doctorate, he was a Research Associate at Boston University's Center for Adaptive Systems until being appointed Assistant Professor of Computer Science and Cognitive and Neural Systems at Boston University. His research interests include computational vision, neural network models, perceptual optics, and parallel computation.

Dejan Todorović is an Assistant Professor in the Department of Psychology at the University of Belgrade, Belgrade, Yugoslavia. He previously completed postdoctoral study at the Center for Adaptive Systems, Boston University, Boston, MA, and the Department of Psychology, University of Connecticut, Storrs. His earlier training was in mathematics and psychology.